Search for the Flavor Changing Neutral Current Decay $t \rightarrow Zq$ in $p\bar{p}$ Collisions at $\sqrt{s} = 1.96$ TeV

T. Aaltonen,[24] J. Adelman,[14] T. Akimoto,[56] M.G. Albrow,[18] B. Álvarez González,[12] S. Amerio[u],[44] D. Amidei,[35] A. Anastassov,[39] A. Annovi,[20] J. Antos,[15] G. Apollinari,[18] A. Apresyan,[49] T. Arisawa,[58] A. Artikov,[16] W. Ashmanskas,[18] A. Attal,[4] A. Aurisano,[54] F. Azfar,[43] P. Azzurri[s],[47] W. Badgett,[18] A. Barbaro-Galtieri,[29] V.E. Barnes,[49] B.A. Barnett,[26] V. Bartsch,[31] G. Bauer,[33] P.-H. Beauchemin,[34] F. Bedeschi,[47] P. Bednar,[15] D. Beecher,[31] S. Behari,[26] G. Bellettini[q],[47] J. Bellinger,[60] D. Benjamin,[17] A. Beretvas,[18] J. Beringer,[29] A. Bhatti,[51] M. Binkley,[18] D. Bisello[u],[44] I. Bizjak,[31] R.E. Blair,[2] C. Blocker,[7] B. Blumenfeld,[26] A. Bocci,[17] A. Bodek,[50] V. Boisvert,[50] G. Bolla,[49] D. Bortoletto,[49] J. Boudreau,[48] A. Boveia,[11] B. Brau,[11] A. Bridgeman,[25] L. Brigliadori,[44] C. Bromberg,[36] E. Brubaker,[14] J. Budagov,[16] H.S. Budd,[50] S. Budd,[25] K. Burkett,[18] G. Busetto[u],[44] P. Bussey[x],[22] A. Buzatu,[34] K. L. Byrum,[2] S. Cabrera[p],[17] C. Calancha,[32] M. Campanelli,[36] M. Campbell,[35] F. Canelli,[18] A. Canepa,[46] D. Carlsmith,[60] R. Carosi,[47] S. Carrillo[j],[19] S. Carron,[34] B. Casal,[12] M. Casarsa,[18] A. Castro[t],[6] P. Catastini[r],[47] D. Cauz[w],[55] V. Cavaliere[r],[47] M. Cavalli-Sforza,[4] A. Cerri,[29] L. Cerrito[n],[31] S.H. Chang,[28] Y.C. Chen,[1] M. Chertok,[8] G. Chiarelli,[47] G. Chlachidze,[18] F. Chlebana,[18] K. Cho,[28] D. Chokheli,[16] J.P. Chou,[23] G. Choudalakis,[33] S.H. Chuang,[53] K. Chung,[13] W.H. Chung,[60] Y.S. Chung,[50] C.I. Ciobanu,[45] M.A. Ciocci[r],[47] A. Clark,[21] D. Clark,[7] G. Compostella,[44] M.E. Convery,[18] J. Conway,[8] K. Copic,[35] M. Cordelli,[20] G. Cortiana[u],[44] D.J. Cox,[8] F. Crescioli[q],[47] C. Cuenca Almenar[p],[8] J. Cuevas[m],[12] R. Culbertson,[18] J.C. Cully,[35] D. Dagenhart,[18] M. Datta,[18] T. Davies,[22] P. de Barbaro,[50] S. De Cecco,[52] A. Deisher,[29] G. De Lorenzo,[4] M. Dell'Orso[q],[47] C. Deluca,[4] L. Demortier,[51] J. Deng,[17] M. Deninno,[6] P.F. Derwent,[18] G.P. di Giovanni,[45] C. Dionisi[v],[52] B. Di Ruzza[w],[55] J.R. Dittmann,[5] M. D'Onofrio,[4] S. Donati[q],[47] P. Dong,[9] J. Donini,[44] T. Dorigo,[44] S. Dube,[53] J. Efron,[40] A. Elagin,[54] R. Erbacher,[8] D. Errede,[25] S. Errede,[25] R. Eusebi,[18] H.C. Fang,[29] S. Farrington,[43] W.T. Fedorko,[14] R.G. Feild,[61] M. Feindt,[27] J.P. Fernandez,[32] C. Ferrazza[s],[47] R. Field,[19] G. Flanagan,[49] R. Forrest,[8] M. Franklin,[23] J.C. Freeman,[18] I. Furic,[19] M. Gallinaro,[52] J. Galyardt,[13] F. Garberson,[11] J.E. Garcia,[47] A.F. Garfinkel,[49] K. Genser,[18] H. Gerberich,[25] D. Gerdes,[35] A. Gessler,[27] S. Giagu[v],[52] V. Giakoumopoulou,[3] P. Giannetti,[47] K. Gibson,[48] J.L. Gimmell,[50] C.M. Ginsburg,[18] N. Giokaris,[3] M. Giordani[w],[55] P. Giromini,[20] M. Giunta[q],[47] G. Giurgiu,[26] V. Glagolev,[16] D. Glenzinski,[18] M. Gold,[38] N. Goldschmidt,[19] A. Golossanov,[18] G. Gomez,[12] G. Gomez-Ceballos,[33] M. Goncharov,[54] O. González,[32] I. Gorelov,[38] A.T. Goshaw,[17] K. Goulianos,[51] A. Gresele[u],[44] S. Grinstein,[23] C. Grosso-Pilcher,[14] R.C. Group,[18] U. Grundler,[25] J. Guimaraes da Costa,[23] Z. Gunay-Unalan,[36] C. Haber,[29] K. Hahn,[33] S.R. Hahn,[18] E. Halkiadakis,[53] B.-Y. Han,[50] J.Y. Han,[50] R. Handler,[60] F. Happacher,[20] K. Hara,[56] D. Hare,[53] M. Hare,[57] S. Harper,[43] R.F. Harr,[59] R.M. Harris,[18] M. Hartz,[48] K. Hatakeyama,[51] J. Hauser,[9] C. Hays,[43] M. Heck,[27] A. Heijboer,[46] B. Heinemann,[29] J. Heinrich,[46] C. Henderson,[33] M. Herndon,[60] J. Heuser,[27] S. Hewamanage,[5] D. Hidas,[17] C.S. Hill[c],[11] D. Hirschbuehl,[27] A. Hocker,[18] S. Hou,[1] M. Houlden,[30] S.-C. Hsu,[10] B.T. Huffman,[43] R.E. Hughes,[40] U. Husemann,[61] J. Huston,[36] J. Incandela,[11] G. Introzzi,[47] M. Iori[v],[52] A. Ivanov,[8] E. James,[18] B. Jayatilaka,[17] E.J. Jeon,[28] M.K. Jha,[6] S. Jindariani,[18] W. Johnson,[8] M. Jones,[49] K.K. Joo,[28] S.Y. Jun,[13] J.E. Jung,[28] T.R. Junk,[18] T. Kamon,[54] D. Kar,[19] P.E. Karchin,[59] Y. Kato,[42] R. Kephart,[18] J. Keung,[46] V. Khotilovich,[54] B. Kilminster,[40] D.H. Kim,[28] H.S. Kim,[28] J.E. Kim,[28] M.J. Kim,[20] S.B. Kim,[28] S.H. Kim,[56] Y.K. Kim,[14] N. Kimura,[56] L. Kirsch,[7] S. Klimenko,[19] B. Knuteson,[33] B.R. Ko,[17] S.A. Koay,[11] K. Kondo,[58] D.J. Kong,[28] J. Konigsberg,[19] A. Korytov,[19] A.V. Kotwal,[17] M. Kreps,[27] J. Kroll,[46] D. Krop,[14] N. Krumnack,[5] M. Kruse,[17] V. Krutelyov,[11] T. Kubo,[56] T. Kuhr,[27] N.P. Kulkarni,[59] M. Kurata,[56] Y. Kusakabe,[58] S. Kwang,[14] A.T. Laasanen,[49] S. Lami,[47] S. Lammel,[18] M. Lancaster,[31] R.L. Lander,[8] K. Lannon,[40] A. Lath,[53] G. Latino[r],[47] I. Lazzizzera[u],[44] T. LeCompte,[2] E. Lee,[54] S.W. Lee[o],[54] S. Leone,[47] J.D. Lewis,[18] C.S. Lin,[29] J. Linacre,[43] M. Lindgren,[18] E. Lipeles,[10] A. Lister,[8] D.O. Litvintsev,[18] C. Liu,[48] T. Liu,[18] N.S. Lockyer,[46] A. Loginov,[61] M. Loreti[u],[44] L. Lovas,[15] R.-S. Lu,[1] D. Lucchesi[u],[44] J. Lueck,[27] C. Luci[v],[52] P. Lujan,[29] P. Lukens,[18] G. Lungu,[51] L. Lyons,[43] J. Lys,[29] R. Lysak,[15] E. Lytken,[49] P. Mack,[27] D. MacQueen,[34] R. Madrak,[18] K. Maeshima,[18] K. Makhoul,[33] T. Maki,[24] P. Maksimovic,[26] S. Malde,[43] S. Malik,[31] G. Manca,[30] A. Manousakis-Katsikakis,[3] F. Margaroli,[49] C. Marino,[27] C.P. Marino,[25] A. Martin,[61] V. Martin[i],[22] M. Martínez,[4] R. Martínez-Ballarín,[32] T. Maruyama,[56] P. Mastrandrea,[52] T. Masubuchi,[56] M.E. Mattson,[59] P. Mazzanti,[6] K.S. McFarland,[50] P. McIntyre,[54] R. McNulty[h],[30] A. Mehta,[30] P. Mehtala,[24] A. Menzione,[47] P. Merkel,[49] C. Mesropian,[51] T. Miao,[18] N. Miladinovic,[7] R. Miller,[36] C. Mills,[23] M. Milnik,[27] A. Mitra,[1] G. Mitselmakher,[19] H. Miyake,[56] N. Moggi,[6] C.S. Moon,[28] R. Moore,[18] M.J. Morello[q],[47] J. Morlok,[27] P. Movilla Fernandez,[18] J. Mülmenstädt,[29] A. Mukherjee,[18] Th. Muller,[27] R. Mumford,[26] P. Murat,[18] M. Mussini[t],[6] J. Nachtman,[18] Y. Nagai,[56] A. Nagano,[56] J. Naganoma,[58] K. Nakamura,[56] I. Nakano,[41] A. Napier,[57] V. Necula,[17] C. Neu,[46] M.S. Neubauer,[25] J. Nielsen[e],[29] L. Nodulman,[2] M. Norman,[10] O. Norniella,[25] E. Nurse,[31] L. Oakes,[43] S.H. Oh,[17]

Y.D. Oh,[28] I. Oksuzian,[19] T. Okusawa,[42] R. Orava,[24] K. Osterberg,[24] S. Pagan Griso[u],[44] C. Pagliarone,[47]
E. Palencia,[18] V. Papadimitriou,[18] A. Papaikonomou,[27] A.A. Paramonov,[14] B. Parks,[40] S. Pashapour,[34]
J. Patrick,[18] G. Pauletta[w],[55] M. Paulini,[13] C. Paus,[33] D.E. Pellett,[8] A. Penzo,[55] T.J. Phillips,[17] G. Piacentino,[47]
E. Pianori,[46] L. Pinera,[19] K. Pitts,[25] C. Plager,[9] L. Pondrom,[60] O. Poukhov,[16] N. Pounder,[43] F. Prakoshyn,[16]
A. Pronko,[18] J. Proudfoot,[2] F. Ptohos[g],[18] E. Pueschel,[13] G. Punzi[q],[47] J. Pursley,[60] J. Rademacker[c],[43]
A. Rahaman,[48] V. Ramakrishnan,[60] N. Ranjan,[49] I. Redondo,[32] B. Reisert,[18] V. Rekovic,[38] P. Renton,[43]
M. Rescigno,[52] S. Richter,[27] F. Rimondi[t],[6] L. Ristori,[47] A. Robson,[22] T. Rodrigo,[12] T. Rodriguez,[46] E. Rogers,[25]
S. Rolli,[57] R. Roser,[18] M. Rossi,[55] R. Rossin,[11] P. Roy,[34] A. Ruiz,[12] J. Russ,[13] V. Rusu,[18] H. Saarikko,[24]
A. Safonov,[54] W.K. Sakumoto,[50] O. Saltó,[4] D. Saltzberg,[9] L. Santi[w],[55] S. Sarkar[v],[52] L. Sartori,[47] K. Sato,[18]
A. Savoy-Navarro,[45] T. Scheidle,[27] P. Schlabach,[18] A. Schmidt,[27] E.E. Schmidt,[18] M.A. Schmidt,[14] M.P. Schmidt[*],[61]
M. Schmitt,[39] T. Schwarz,[8] L. Scodellaro,[12] A.L. Scott,[11] A. Scribano[r],[47] F. Scuri,[47] A. Sedov,[49] S. Seidel,[38]
Y. Seiya,[42] A. Semenov,[16] L. Sexton-Kennedy,[18] A. Sfyrla,[21] S.Z. Shalhout,[59] T. Shears,[30] P.F. Shepard,[48]
D. Sherman,[23] M. Shimojima[l],[56] S. Shiraishi,[14] M. Shochet,[14] Y. Shon,[60] I. Shreyber,[37] A. Sidoti,[47] P. Sinervo,[34]
A. Sisakyan,[16] A.J. Slaughter,[18] J. Slaunwhite,[40] K. Sliwa,[57] J.R. Smith,[8] F.D. Snider,[18] R. Snihur,[34] A. Soha,[8]
S. Somalwar,[53] V. Sorin,[36] J. Spalding,[18] T. Spreitzer,[34] P. Squillacioti[r],[47] M. Stanitzki,[61] R. St. Denis,[22]
B. Stelzer,[9] O. Stelzer-Chilton,[43] D. Stentz,[39] J. Strologas,[38] D. Stuart,[11] J.S. Suh,[28] A. Sukhanov,[19]
M. Sutherland,[9] I. Suslov,[16] T. Suzuki,[56] A. Taffard[d],[25] R. Takashima,[41] Y. Takeuchi,[56] R. Tanaka,[41]
M. Tecchio,[35] P.K. Teng,[1] K. Terashi,[51] J. Thom[f],[18] A.S. Thompson,[22] G.A. Thompson,[25] E. Thomson,[46]
P. Tipton,[61] V. Tiwari,[13] S. Tkaczyk,[18] D. Toback,[54] S. Tokar,[15] K. Tollefson,[36] T. Tomura,[56] D. Tonelli,[18]
S. Torre,[20] D. Torretta,[18] P. Totaro[w],[55] S. Tourneur,[45] Y. Tu,[46] N. Turini[r],[47] F. Ukegawa,[56] S. Vallecorsa,[21]
N. van Remortel[a],[24] A. Varganov,[35] E. Vataga[s],[47] F. Vázquez[j],[19] G. Velev,[18] C. Vellidis,[3] V. Veszpremi,[49]
M. Vidal,[32] R. Vidal,[18] I. Vila,[12] R. Vilar,[12] T. Vine,[31] M. Vogel,[38] I. Volobouev[o],[29] G. Volpi[q],[47] F. Würthwein,[10]
P. Wagner,[2] R.G. Wagner,[2] R.L. Wagner,[18] J. Wagner-Kuhr,[27] W. Wagner,[27] T. Wakisaka,[42] R. Wallny,[9]
S.M. Wang,[1] A. Warburton,[34] D. Waters,[31] M. Weinberger,[54] W.C. Wester III,[18] B. Whitehouse,[57] D. Whiteson[d],[46]
A.B. Wicklund,[2] E. Wicklund,[18] G. Williams,[34] H.H. Williams,[46] P. Wilson,[18] B.L. Winer,[40] P. Wittich[f],[18]
S. Wolbers,[18] C. Wolfe,[14] T. Wright,[35] X. Wu,[21] S.M. Wynne,[30] A. Yagil,[10] K. Yamamoto,[42] J. Yamaoka,[53]
U.K. Yang[k],[14] Y.C. Yang,[28] W.M. Yao,[29] G.P. Yeh,[18] J. Yoh,[18] K. Yorita,[14] T. Yoshida,[42] G.B. Yu,[50] I. Yu,[28]
S.S. Yu,[18] J.C. Yun,[18] L. Zanello[v],[52] A. Zanetti,[55] I. Zaw,[23] X. Zhang,[25] Y. Zheng[b],[9] and S. Zucchelli[t][6]

(CDF Collaboration[†])

The CDF Collaboration

[1]*Institute of Physics, Academia Sinica, Taipei, Taiwan 11529, Republic of China*
[2]*Argonne National Laboratory, Argonne, Illinois 60439*
[3]*University of Athens, 157 71 Athens, Greece*
[4]*Institut de Fisica d'Altes Energies, Universitat Autonoma de Barcelona, E-08193, Bellaterra (Barcelona), Spain*
[5]*Baylor University, Waco, Texas 76798*
[6]*Istituto Nazionale di Fisica Nucleare Bologna, [t]University of Bologna, I-40127 Bologna, Italy*
[7]*Brandeis University, Waltham, Massachusetts 02254*
[8]*University of California, Davis, Davis, California 95616*
[9]*University of California, Los Angeles, Los Angeles, California 90024*
[10]*University of California, San Diego, La Jolla, California 92093*
[11]*University of California, Santa Barbara, Santa Barbara, California 93106*
[12]*Instituto de Fisica de Cantabria, CSIC-University of Cantabria, 39005 Santander, Spain*
[13]*Carnegie Mellon University, Pittsburgh, PA 15213*
[14]*Enrico Fermi Institute, University of Chicago, Chicago, Illinois 60637*
[15]*Comenius University, 842 48 Bratislava, Slovakia; Institute of Experimental Physics, 040 01 Kosice, Slovakia*
[16]*Joint Institute for Nuclear Research, RU-141980 Dubna, Russia*
[17]*Duke University, Durham, North Carolina 27708*
[18]*Fermi National Accelerator Laboratory, Batavia, Illinois 60510*
[19]*University of Florida, Gainesville, Florida 32611*
[20]*Laboratori Nazionali di Frascati, Istituto Nazionale di Fisica Nucleare, I-00044 Frascati, Italy*
[21]*University of Geneva, CH-1211 Geneva 4, Switzerland*
[22]*Glasgow University, Glasgow G12 8QQ, United Kingdom*
[23]*Harvard University, Cambridge, Massachusetts 02138*
[24]*Division of High Energy Physics, Department of Physics,*
University of Helsinki and Helsinki Institute of Physics, FIN-00014, Helsinki, Finland
[25]*University of Illinois, Urbana, Illinois 61801*
[26]*The Johns Hopkins University, Baltimore, Maryland 21218*
[27]*Institut für Experimentelle Kernphysik, Universität Karlsruhe, 76128 Karlsruhe, Germany*

[28] Center for High Energy Physics: Kyungpook National University,
Daegu 702-701, Korea; Seoul National University, Seoul 151-742,
Korea; Sungkyunkwan University, Suwon 440-746,
Korea; Korea Institute of Science and Technology Information, Daejeon,
305-806, Korea; Chonnam National University, Gwangju, 500-757, Korea
[29] Ernest Orlando Lawrence Berkeley National Laboratory, Berkeley, California 94720
[30] University of Liverpool, Liverpool L69 7ZE, United Kingdom
[31] University College London, London WC1E 6BT, United Kingdom
[32] Centro de Investigaciones Energeticas Medioambientales y Tecnologicas, E-28040 Madrid, Spain
[33] Massachusetts Institute of Technology, Cambridge, Massachusetts 02139
[34] Institute of Particle Physics: McGill University, Montréal,
Canada H3A 2T8; and University of Toronto, Toronto, Canada M5S 1A7
[35] University of Michigan, Ann Arbor, Michigan 48109
[36] Michigan State University, East Lansing, Michigan 48824
[37] Institution for Theoretical and Experimental Physics, ITEP, Moscow 117259, Russia
[38] University of New Mexico, Albuquerque, New Mexico 87131
[39] Northwestern University, Evanston, Illinois 60208
[40] The Ohio State University, Columbus, Ohio 43210
[41] Okayama University, Okayama 700-8530, Japan
[42] Osaka City University, Osaka 588, Japan
[43] University of Oxford, Oxford OX1 3RH, United Kingdom
[44] Istituto Nazionale di Fisica Nucleare, Sezione di Padova-Trento, [u] University of Padova, I-35131 Padova, Italy
[45] LPNHE, Universite Pierre et Marie Curie/IN2P3-CNRS, UMR7585, Paris, F-75252 France
[46] University of Pennsylvania, Philadelphia, Pennsylvania 19104
[47] Istituto Nazionale di Fisica Nucleare Pisa, [q] University of Pisa,
[r] University of Siena and [s] Scuola Normale Superiore, I-56127 Pisa, Italy
[48] University of Pittsburgh, Pittsburgh, Pennsylvania 15260
[49] Purdue University, West Lafayette, Indiana 47907
[50] University of Rochester, Rochester, New York 14627
[51] The Rockefeller University, New York, New York 10021
[52] Istituto Nazionale di Fisica Nucleare, Sezione di Roma 1,
[v] Sapienza Università di Roma, I-00185 Roma, Italy
[53] Rutgers University, Piscataway, New Jersey 08855
[54] Texas A&M University, College Station, Texas 77843
[55] Istituto Nazionale di Fisica Nucleare Trieste/ Udine, [w] University of Trieste/ Udine, Italy
[56] University of Tsukuba, Tsukuba, Ibaraki 305, Japan
[57] Tufts University, Medford, Massachusetts 02155
[58] Waseda University, Tokyo 169, Japan
[59] Wayne State University, Detroit, Michigan 48201
[60] University of Wisconsin, Madison, Wisconsin 53706
[61] Yale University, New Haven, Connecticut 06520
(Dated: May 7, 2008)

We report a search for the flavor changing neutral current (FCNC) decay of the top quark $t \to Zq$ ($q = u, c$) in $p\bar{p}$ collisions at $\sqrt{s} = 1.96$ TeV using a data sample corresponding to an integrated luminosity of 1.9 fb^{-1} collected by the CDF II detector. This decay is strongly suppressed in the standard model (SM) and a signal at the Tevatron would be an indication of physics beyond the SM. Using $Z+ \geq 4$ jet final state candidate events, both with and without an identified bottom quark jet, we discriminate signal from background by exploring kinematic constraints present in FCNC events and obtain an upper limit of $\mathcal{B}(t \to Zq) < 3.7\%$ at 95% C.L.

[*] Deceased
[†] With visitors from [a] Universiteit Antwerpen, B-2610 Antwerp, Belgium, [b] Chinese Academy of Sciences, Beijing 100864, China, [c] University of Bristol, Bristol BS8 1TL, United Kingdom, [d] University of California Irvine, Irvine, CA 92697, [e] University of California Santa Cruz, Santa Cruz, CA 95064, [f] Cornell University, Ithaca, NY 14853, [g] University of Cyprus, Nicosia CY-1678, Cyprus, [h] University College Dublin, Dublin 4, Ireland, [i] University of Edinburgh, Edinburgh EH9 3JZ, United Kingdom, [j] Universidad Iberoamericana, Mexico D.F., Mexico, [k] University of Manchester, Manchester M13 9PL, England, [l] Nagasaki Institute of Applied Science, Nagasaki, Japan, [m] University de Oviedo, E-33007 Oviedo, Spain, [n] Queen Mary, University of London, London, E1 4NS, England, [o] Texas Tech University, Lubbock, TX 79409, [p] IFIC(CSIC-Universitat de Valencia), 46071 Valencia, Spain, [x] Royal Society of Edinburgh/Scottish Executive Support Research Fellow,

FCNC interactions, which are suppressed in the SM, are sensitive indicators of physics beyond the SM (BSM). Presently there are only loose experimental bounds on FCNC decays of the top quark [1], the heaviest quark in the SM. While the SM branching fraction for $t \to Zq$ ($q = u, c$) is predicted to be $\mathcal{O}(10^{-14})$ [2], many BSM models such as supersymmetry and quark compositeness allow for a much higher branching fraction, up to $\mathcal{O}(10^{-4})$ [2, 3]. Any observation of the top FCNC decay $t \to Zq$ at the Tevatron would be an indication of BSM physics.

In Run I, the CDF search for the $t \to Zq$ decay yielded an upper limit on the branching fraction $\mathcal{B}(t \to Zq)$ of 33% at 95% C.L. [4]. The current best 95% C.L. upper limit on $\mathcal{B}(t \to Zq)$, 13.7%, was set by the L3 experiment [5] from the non-observation of FCNC single top quark production. For these analyses and this Letter, a top quark mass of 175 GeV/c^2 is assumed.

We present the first Tevatron Run II search for the top FCNC decay $t \to Zq$ in events with a Z boson and four or more jets. In these events, one of the top quarks can decay via an FCNC to a Z boson and a quark (u or c), and the other top quark undergoes the SM decay $t \to Wb$. We examine the decay channel in which the Z subsequently decays to a pair of charged leptons (e^+e^- or $\mu^+\mu^-$), and the W decays to two quarks. The search allows events in which both top quarks decay via FCNC and takes into account their impact on the signal acceptance. The data sample analyzed for this Letter corresponds to an integrated luminosity of 1.9 fb^{-1} of $p\bar{p}$ collisions at $\sqrt{s} = 1.96$ TeV, collected by the CDF II detector from March 2002 to May 2007.

The components of the CDF II detector relevant to this analysis are briefly described here; a more complete description can be found elsewhere [6]. The transverse momenta p_T and pseudorapidities η [7] of charged particles are measured by a silicon strip detector [8] and a 96-layer drift chamber (COT) [9] inside a 1.4 T solenoidal magnetic field. The silicon detector and the COT provide good combined reconstruction efficiency for $|\eta| < 1.2$. The precise position resolution of the silicon detector is also crucial for identifying displaced secondary vertices from b hadrons. Electromagnetic (EM) and hadronic calorimeters surround the tracking system. They are segmented in a projective tower geometry and measure energies of charged and neutral particles in the central ($|\eta| < 1.1$) and end-plug ($1.1 < |\eta| < 3.6$) regions. Four layers of planar drift chambers located on the rear of the central hadron calorimeters and another set behind a 60 cm thick steel absorber detect muons with $|\eta| < 0.6$. Additional drift chambers and scintillation counters detect muons in the region $0.6 < |\eta| < 1.0$. Gas Cherenkov counters [10] measure the average number of inelastic $p\bar{p}$ collisions per bunch crossing and thereby determine the luminosity. A three level trigger selects events that contain electrons (muons) with $E_T > 18$ GeV ($p_T > 18$ GeV/c) as required in this analysis.

Our base selection chooses events with two oppositely-charged electrons or muons of the same flavor and four or more jets. One lepton is required to be a central electron

or muon, the other can be a forward electron or a track, as described below. The leptons must be compatible with originating from a Z boson in the mass window from 76 GeV/c^2 to 106 GeV/c^2.

All leptons used in this analysis are required to be well isolated in a cone of $\Delta R = \sqrt{(\Delta\eta)^2 + (\Delta\phi)^2} < 0.4$ [7] and to have transverse energies E_T (momenta p_T) greater than 20 GeV (20 GeV/c). Electrons are identified by requiring an energy cluster in the EM calorimeter with a single track pointing to it. Central electrons are required to have a high quality COT-based track, calorimeter cluster E_T consistent with the track p_T, a high fraction of the total energy deposition in the EM calorimeter, and a lateral shower profile consistent with electron showers. Forward electrons are reconstructed in the end-plug calorimeter and have similar constraints except that the tracks are reconstructed only in the silicon detector and the calorimeter cluster E_T and track p_T are not compared. Muons are identified by matching tracks reconstructed in the COT to track segments reconstructed in the muon chambers and by requiring energy depositions in the calorimeters consistent with minimum ionizing particles. The muons in this analysis are required to be in the central region ($|\eta| < 1.0$). We double the acceptance for leptonic Z decays relative to the above electron and muon selection by also allowing isolated tracks which pass COT and silicon detector track quality cuts to be lepton candidates. For tracks used as electrons, if an EM calorimeter tower is associated to the track and the energy of the EM tower is greater than the track momentum, the EM tower energy is used instead of the track momentum.

Jets are identified by energy deposited in the calorimeters within a cone of $\Delta R < 0.4$. To recover the true parton energy, jets are corrected for instrumental effects [11]. We select events with at least four jets with corrected $E_T > 15$ GeV and $|\eta| < 2.4$. The SecVtx algorithm [6] is used for identifying displaced secondary vertices from long-lived b hadrons ("b-tagging").

We use the PYTHIA v6.216 Monte Carlo (MC) generator [13] to simulate FCNC signal in $t\bar{t}$ events and all sources of SM background except the production of Z bosons with associated jets (Z+jets). We employ the ALPGEN MC generator [14], version 2.10$'$ interfaced to PYTHIA v6.325, to simulate kinematic distributions of Z+jets events. Acceptance, efficiency, and kinematic distributions of the $t \to Zq$ signal are determined from the above MC simulations. We add a $t \to Zq$ decay channel to PYTHIA by forcing the Z helicity to be consistent with the expectation from an SM-like Higgs mechanism of 65% longitudinally polarized and 35% left-handed Z bosons. The 15% relative difference between the largest signal acceptance (100% longitudinal Z) and the smallest signal acceptance (100% left- or right-handed Z) is taken as a systematic uncertainty. The main signal MC sample contains events with a $t\bar{t}$ pair, so that one of the top quarks decays via the FCNC decay mode $t \to Zc$, and the other via the SM decay mode, $t \to Wb$. If the $t \to Zc$ decay is replaced by $t \to Zu$, the probability to

b-tag an FCNC signal event drops by 9%, which is taken into account as a systematic uncertainty. The Z boson decays to leptons, and the W boson to a quark and an anti-quark. To cover the full signal acceptance, we have generated an additional sample in which both top quarks decay via the FCNC mode and the Z is allowed to decay into the e^+e^-, $\mu^+\mu^-$, and $q\bar{q}$ decay modes. The relative amount of $t\bar{t} \to WbZc$ to $t\bar{t} \to ZcZc$ is adjusted according to the branching fraction $\mathcal{B}(t \to Zq)$ during the limit calculation. For systematic studies, we have also generated a sample in which the W and Z bosons can decay to all allowed decay products. We apply corrections for trigger efficiencies and for different efficiencies in data and simulation for lepton identification and reconstruction, b-tagging, and misidentification of secondary vertices (mistags).

To determine the FCNC branching fraction, we take into account single or double FCNC decays of $t\bar{t}$ pairs and normalize to the SM $t\bar{t}$ event yield in the decay mode $t\bar{t} \to WbWb \to \ell\nu b\,q\bar{q}'b$ ("lepton+jets") requiring at least two jets to be secondary vertex b-tagged [15]. We observe a number of $t\bar{t}$ candidate events consistent with a production cross section of 8.8 ± 0.7 (stat.) pb assuming a branching fraction of $\mathcal{B}(t \to Wb) = 100\%$. If $t \to Zq$ decays were present, these additional $t\bar{t}$ decays are less likely to be reconstructed in the lepton+jets mode, resulting in a measured $t\bar{t}$ production cross section smaller than the actual cross section. We correct for this effect by modifying the measured cross section based on the limit we set on $\mathcal{B}(t \to Zq)$. Normalization to the lepton+jets event yields in the $t\bar{t}$ production cross section analysis removes nearly all uncertainties depending directly on luminosity. Many other systematic uncertainties also partially cancel. We absorb the statistical and systematic uncertainties of the $t\bar{t}$ production cross section measurement as part of the systematic uncertainty (7.8%).

Several SM processes result in final states with a reconstructed Z boson and four or more jets. SM Z+jets production is by far the largest background and the most difficult to estimate; therefore the number of Z+jets events is determined by a fit to the data. A small contribution to the background results from SM $t\bar{t} \to W^+bW^-\bar{b}$ events. SM $t\bar{t}$ decays do not contain real Z bosons; however, dilepton masses within the Z mass window can be reconstructed both in the dilepton decay mode $t\bar{t} \to WbWb \to \ell\nu b\ell\nu b$ and in the lepton+jets decay mode when one of the jets is reconstructed as a lepton. Although SM $t\bar{t}$ decays contribute only a small fraction of the background, the presence of two b-jets increases their probability to contain one or more secondary vertex b-tags. The production of a pair of gauge bosons (dibosons), WZ and ZZ, contributes an additional small number of background events. The background contributions from WW diboson production and from W bosons produced in association with jets are negligible. All of the smaller backgrounds are estimated using MC simulations. The SM $t\bar{t}$ background is normalized to the observed event yield in the lepton+jets decay mode; backgrounds from diboson production are normalized to their theoretical cross sections. The total expected background from SM $t\bar{t}$ production and diboson production is 11 ± 1 events.

The decay $t\bar{t} \to WbZq \to q\bar{q}'b\,\ell\ell q''$ contains no high-energy neutrinos; therefore we can fully reconstruct the event kinematics. The four jets in signal events result from the b quark, the decay products of the W from the $t \to Wb$ decay, and the c or u quark from the $t \to Zq$ decay. We form all permutations of the four leading (highest transverse energy) jets in the events to compare the reconstructed masses (m_{rec}) of the W, top quark decaying to Wb, and top quark decaying to Zq. We define a mass χ^2 as

$$\chi^2 = \left(\frac{m_{W,\mathrm{rec}} - m_W}{\sigma_W}\right)^2 + \left(\frac{m_{t\to Wb,\mathrm{rec}} - m_t}{\sigma_{t\to Wb}}\right)^2 + \left(\frac{m_{t\to Zq,\mathrm{rec}} - m_t}{\sigma_{t\to Zq}}\right)^2, \quad (1)$$

and select the permutation with the smallest χ^2. We scale the measured four-momenta of the W and Z boson daughter particles such that the boson masses are fixed to the world average values [12] and use the scaled four-momenta to calculate the two top quark masses. The widths used are given by the standard deviations of the reconstructed masses measured in the MC simulation of FCNC events. Using the correct pairing of jets to partons, we extract $\sigma_W = 15$ GeV/c^2, $\sigma_{t\to Wb} = 24$ GeV/c^2, and $\sigma_{t\to Zq} = 21$ GeV/c^2.

Since our FCNC signal events originate from $t\bar{t}$ decays, they contain more central Z bosons and jets than background events. To exploit this, we use the transverse mass of the Z and the four leading jets, defined as $m_T = \sqrt{\left(\sum E_T\right)^2 - \left(\sum \vec{p}_T\right)^2}$, as a selection criterion. We also apply a tiered cut on the transverse momenta of the four leading jets, as FCNC signal events contain jets with higher transverse momenta than SM background events.

Using the first 1.1 fb^{-1} of integrated luminosity, we performed a blind counting experiment [17] selection optimized with mass χ^2, m_T, and the transverse energies of the four leading jets. We leave the optimized selection unchanged after unblinding and apply it to the full 1.9 fb^{-1} result. This selection requires two oppositely-charged leptons of the same flavor and a mass between 76 GeV/c^2 and 106 GeV/c^2, with the leading jet $E_T \geq 40$ GeV, second jet $E_T \geq 30$ GeV, third jet $E_T \geq 20$ GeV, and fourth jet $E_T \geq 15$ GeV, and transverse mass $m_T \geq 200$ GeV/c^2. After optimization, 88% of the FCNC signal events remain, compared to 33% of the background events. All events that pass the optimized selection are further divided into two regions based on whether any of the four leading jets has an identified b-jet ("b-tagged region") or not ("non-b-tagged region"); those events that pass the base selection but not the optimized selection above are placed in a "control" region. The inclusive signal acceptances for the decay $t\bar{t} \to WbZc$ ($t\bar{t} \to ZcZc$) are 0.43% (0.58%) for the b-tagged selection, 0.34% (0.86%) for the non-b-tagged selection, and 0.10% (0.16%) for the control region.

We extract a limit on the branching fraction $\mathcal{B}(t \to Zq)$ from a fit to the mass χ^2 distribution using templates constructed from the MC simulated mass χ^2 distributions of the FCNC signal and the SM backgrounds (Z+jets, SM $t\bar{t}$, and dibosons). The b-tagged, the non-b-tagged, and the control region are fit simultaneously. We include systematic uncertainties due to the shapes of the signal and background templates by allowing the templates to change shape via a histogram interpolation technique (horizontal template morphing) [18]. The experimental jet energy scale (JES) is the largest source of shape uncertainties, and the data are most consistent with a shift of the JES; therefore we only include JES induced shape uncertainties in the fitting procedure. To account for shape uncertainties that are not due to JES, we measure the bias on the fitted branching fraction $\mathcal{B}(t \to Zq)$ in simulated experiments generated assuming the second largest source of shape uncertainties, the MC generator used for the Z+jets background. We simulate Z+jets events for which the vertex energy scale is varied by factors of two. The estimated bias of 0.2% is included as a systematic uncertainty.

While only 12% of FCNC signal acceptance falls in the control region (as compared to the base selection), two-thirds of the SM backgrounds are located there; therefore the control region can be used to constrain the background shape uncertainties without losing sensitivity to a small FCNC signal. Additionally we use the number of Z+jets events observed in the control region, Z_{control}, to place a loose constraint on the number of Z+jets events in the two signal regions, Z_{signal}. We constrain the ratio $\mathcal{R}_{\text{sig}} = Z_{\text{signal}}/Z_{\text{control}}$ to the value estimated by the MC simulation, $\mathcal{R}_{\text{sig}} = 0.51 \pm 0.10$ at the nominal JES. The uncertainty is conservatively estimated by varying the energy scales in the ALPGEN MC generator as described above. We adjust $\mathcal{R}_{\text{sig}}$ as a function of the JES shift σ_{JES}, keeping the relative uncertainty of 20%. The absolute number of Z+jets background events remains unconstrained. To reflect the constraint on $\mathcal{R}_{\text{sig}}$ in the template fit, we parameterize the number of Z+jets events passing the b-tagged and non-b-tagged signal selections, Z_{tagged} and $Z_{\text{non-tagged}}$, as $Z_{\text{tagged}} = f_{\text{tag}} \cdot \mathcal{R}_{\text{sig}} \cdot Z_{\text{control}}$ and $Z_{\text{non-tagged}} = (1 - f_{\text{tag}}) \cdot \mathcal{R}_{\text{sig}} \cdot Z_{\text{control}}$, where f_{tag} is the fraction of Z+jets events passing the b-tagged signal selection. In summary, the unconstrained parameters of the template fit include the branching fraction $\mathcal{B}(t \to Zq)$, Z_{control}, the tagging fraction f_{tag}, and the shift in JES σ_{JES}. We apply a Gaussian constraint on the ratio $\mathcal{R}_{\text{sig}}$. The templates for the smaller backgrounds, SM $t\bar{t}$ and diboson production, are fixed in the fit.

In addition to the template shape uncertainties, we assign systematic uncertainties on the MC predictions of the signal acceptance and the background rates. The uncertainties are divided into anti-correlated uncertainties, those which cause migration of events between b-tagged and non-b-tagged selections, and correlated uncertainties, those which simultaneously increase or decrease both selections.

The signal acceptance systematic uncertainties are

TABLE I: Results of the fit to data. From the ratio of the number of Z+jets events in the signal and the control regions and the tagging fraction f_{tag}, we obtain $Z_{\text{tagged}} = 13.5$ events and $Z_{\text{non-tagged}} = 53.9$ events.

Fit Parameter	Value		
Branching Fraction, $\mathcal{B}(t \to Zq)$ (%)	-1.49	$\pm$	1.52
Z+Jets Events in Control Region, Z_{control}	129.0	$\pm$	11.1
Ratio Signal/Control Region, $\mathcal{R}_{\text{sig}}$	0.52	$\pm$	0.07
Tagging Fraction, f_{tag}	0.20	$\pm$	0.06
Jet Energy Scale Shift, σ_{JES}	-0.74	$\pm$	0.43

evaluated for the ratio of the FCNC signal acceptance to the acceptance for the event selection used in our normalization process, $t\bar{t}$ production in the lepton+jets channel. The sources of correlated signal acceptance systematic uncertainty are the helicity of the Z from $t \to Zq$ decays, initial and final state radiation, lepton identification and reconstruction scale factors, trigger efficiency, and choice of parton distribution functions, resulting in a total correlated relative systematic uncertainty of (6.1%) 6.2% for the (non-)b-tagged selection and 5.9% for the control region. Acceptance uncertainties due to the choice of the JES scale are already taken into account as uncertainties of the template shape. The sources of anti-correlated signal acceptance systematic uncertainty are b-tagging scale factor, b-tagging efficiency difference for the decay $t \to Zc$ versus the decay $t \to Zu$, and mistag parameterization correction, resulting in a total correlated systematic uncertainty of (16.7%) 7.2% for the (non-)b-tagged event selection and 10.2% for the control region.

Background rate uncertainties affect only the smaller SM $t\bar{t}$ and diboson backgrounds. The rate of the dominant Z+jets background in the control region is a free parameter in the template fit; therefore we do not assign systematic uncertainties for this. The sources of correlated background rate uncertainty include luminosity, lepton identification and reconstruction scale factors, and trigger efficiency; the total correlated uncertainty is 6.2% for the b-tagged selection, for the non-b-tagged selection, and for the control region. The sources of anti-correlated background rate uncertainty are b-tagging scale factor and mistag parameterization correction, resulting in a (2.5%) 3.2% systematic uncertainty for the (non-)b-tagged selection.

We employ a Feldman-Cousins (FC) limit calculation framework that includes the handling of systematic uncertainties [16]. The FC construction is based on applying the above template fits to simulated experiments that are generated taking into account all known sources of systematic rate and shape uncertainty and their correlations. We expect a limit of (5.0 ± 2.2)% in the absence of signal. The results of the template fit to the data are shown in Table I and in Fig. 1. From the fit we measure a branching fraction $\mathcal{B}(t \to Zq) = -1.49$% and find an upper limit of 3.7% at 95% C.L.

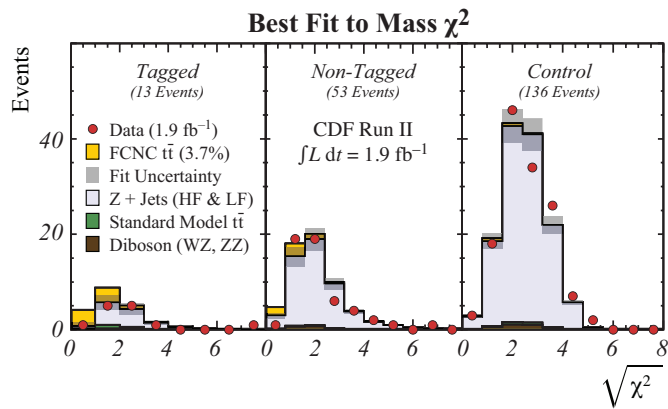In conclusion, we have searched for the top quark flavor changing neutral current decay $t \to Zq$ in events with

Best Fit to Mass χ²

FIG. 1: Mass χ^2 distribution for b-tagged and non-b-tagged signal regions and the control region. The data points as a function of $\sqrt{\chi^2}$ are compared to the SM background prediction and the expected FCNC yield at the observed 95% C.L. upper limit on the $t \to Zq$ branching fraction $\mathcal{B}(t \to Zq) < 3.7\%$. The data are consistent with the background prediction.

a Z boson and four or more jets using CDF Run II data corresponding to 1.9 fb^{-1} of integrated luminosity. The data are consistent with the SM background prediction, and we set an upper limit on the branching fraction

$\mathcal{B}(t \to Zq)$ of 3.7% at 95% C.L. at a top quark mass of 175 GeV/c^2. Assuming a top quark mass of 170 GeV/c^2, the 95% C.L. upper limit is 4.1%. Compared with the previous world's best limit of 13.7% by the L3 experiment [5] at LEP2, and the previous Tevatron upper limit of 33%, as reported by CDF Run I [4], our reported limit of 3.7% represents a substantial improvement.

[1] H. Fritzsch, Phys. Lett. B **224**, 423 (1989).
[2] J. A. Aguilar-Saavedra, Acta Phys. Polon. B **35**, 2695 (2004).
[3] F. Larios, R. Martínez, M.A. Pérez, Int. J. Mod. Phys. A **21**, 3473 (2006).
[4] F. Abe *et al.* (CDF Collaboration), Phys. Rev. Lett. **80**, 2525 (1998).
[5] P. Achard *et al.* (L3 Collaboration), Phys. Lett. B **549**, 290 (2002).
[6] D. Acosta *et al.* (CDF Collaboration), Phys. Rev. D **71**, 052003 (2005).
[7] In the CDF geometry, θ is the polar angle with respect to the proton beam axis (positive z direction), and ϕ is the azimuthal angle. The pseudorapidity is $\eta = -\ln[\tan(\theta/2)]$.
[8] A. Sill *et al.*, Nucl. Instrum. Methods A **447**, 1 (2000). T. Affolder *et al.*, Nucl. Instrum. Methods A **453**, 84 (2000). C.S. Hill *et al.*, Nucl. Instrum. Methods A **511**, 118 (2003).
[9] T. Affolder *et al.*, Nucl. Instrum. Methods A **526**, 249 (2004).
[10] D. Acosta *et al.*, Nucl. Instrum. Methods A **461**, 540 (2001).
[11] A. Bhatti *et al.*, Nucl. Instrum. Methods A **566**, 2 (2006).
[12] W.-M. Yao *et al.*, J. Phys. G **33**, 1 (2006).
[13] T. Sjöstrand *et al.*, Comput. Phys. Commun. **135**, 238 (2001).
[14] M. L. Mangano *et al.*, JHEP **07**, 001 (2003).
[15] D. Sherman, Ph.D. Thesis, Harvard University (2007).
[16] D. Acosta *et al.*, Phys. Rev. Lett. **95**, 102002 (2005).
[17] For the 1.1 fb^{-1} blind analysis, we obtain a 95% C.L. limit of $\mathcal{B}(t \to Zq) < 10.4\%$ (expected limit: 6.8%), consistent with a 1σ upward fluctuation of the expected SM backgrounds.
[18] A. L. Read, Nucl. Instrum. Methods A **425**, 357 (1999).